JOURNAL OF AGRICULTURAL AND FOOD CHEMISTRY

Article

pubs.acs.org/JAFC

Collagen Fibril Alignment and Deformation during Tensile Strain of Leather: A Small-Angle X-ray Scattering Study

Melissa M. Basil-Jones,[†] Richard L. Edmonds,[‡] Gillian E. Norris,[§] and Richard G. Haverkamp*[,†]

[†]School of Engineering and Advanced Technology, and [§]Institute of Molecular Biosciences, Massey University, Palmerston North 4442, New Zealand

[‡]Leather and Shoe Research Association, Palmerston North 4442, New Zealand

ABSTRACT: The distribution and effect of applied strain on the collagen fibrils that make up leather may have an important bearing on the ultimate strength and other physical properties of the material. While sections of ovine and bovine leather were being subjected to tensile strain up to rupture, synchrotron-based small-angle X-ray scattering (SAXS) spectra were recorded edge-on to the leather at points from the corium to the grain. Measurements of both fibril orientation and collagen *d* spacing showed that, initially, the fibers reorient under strain, becoming more aligned. As the strain increases (5−10% strain), further fibril reorientation diminishes until, at 37% strain, the *d* spacing increases by up to 0.56%, indicating that significant tensile forces are being transmitted to individual fibrils. These changes, however, are not uniform through the cross-section of leather and differ between leathers of different strengths. The stresses are taken up more evenly through the leather cross-section in stronger leathers in comparison to weaker leathers, where stresses tended to be concentrated during strain. These observations contribute to our understanding of the internal strains and structural changes that take place in leather under stress.

KEYWORDS: *Collagen, SAXS, tissue, skin, synchrotron*

INTRODUCTION

Leather is a remarkable biomaterial that exhibits strength, wear, and aesthetic properties that are hard to match with synthetic materials.[1] It is composed mostly of collagen fibrils that are arranged in a way that confers strength to the material. As a treated form of animal skin, leather is structurally similar to the skin of animals and humans in its natural state[2] and to some other tissues in animals, such as pericardium, cartilage, and tendon. Processed biomaterials, such as the extracellular matrix of ovine forestomach used for tissue regeneration, also have a similar structure.[3]

Ovine leather is weaker than bovine leather of the same thickness, typically half of the strength, making ovine leather a low-value product relative to bovine leather. Previously, we showed how small-angle X-ray scattering (SAXS) investigations of leather can provide detailed structural information on the amount of fibrous collagen, the microfibril orientation, and the *d* spacing.[4] We then showed that there is a correlation between the tear strength in ovine and bovine leather and the orientation of collagen microfibrils in those leathers. Stronger leather is found to have more fibrils aligned with the surface of the leather, with less crossover between layers, than weak leather (i.e., strong leather had a lower angle of weave).[5]

Previous studies have also used SAXS to investigate the structure of collagenous materials, such as those found in tendons,[6,7] bone,[8,9] ligaments,[10] human articular cartilages,[11] breast tissue,[12] mitral valve leaflets,[13] and materials for tissue regeneration scaffolds.[3]

SAXS has also been used to study collagenous materials under tension where changes in *d* spacing[7,14] and orientation[15] have been observed. The building blocks of collagen are pro-collagen molecules, with each one a repeating sequence of (glycine−X−Y)$_n$, where X and Y can be any amino acid and n is the number of repeats (usually 100−400). Three pro-collagen molecules arrange in a coiled coil to form a collagen molecule. Several collagen molecules aligned in a quarter-staggered array form a collagen microfibril, which has overlap and gap regions, giving rise to a banding pattern visible by scanning electron microscopy (SEM) or atomic force microscopy (AFM). The distance between these bands is referred to as the *d* spacing and may be obtained from the diffraction pattern.

Leather has been subjected to biaxial stretching and monitored with wide-angle X-ray scattering (WAXS)[16] to observe changes to the fiber orientation measured both normal to the surface and normal to the edge. This study showed an increase in fibril orientation measured normal to the edge during stretching. Another technique, small-angle light scattering, has been used to monitor the effects of collagen fiber orientation during the stretching of bovine pericardium tissue, demonstrating increased fiber alignment when tissue is stretched in parallel to the dominant fiber direction.[17]

In this work, we investigate the changes that take place in the microstructure of leather as a strain is applied, particularly in the direction edge-on to the leather. The objectives of the study are to obtain physical data that can be related to the deformation and failure mechanism of the material. The results will identify physical differences between weak and strong leather and between ovine and bovine leather. They will thus inform the development of new processes to modify ovine leather to better accommodate strain and, therefore, to increase the tear strength to improve the value of the material.

Received: September 29, 2011
Revised: January 5, 2012
Accepted: January 10, 2012
Published: January 10, 2012

■ EXPERIMENTAL SECTION

Ovine pelts were from 5-month-old, early season lambs of breeds with "black face" lambs, which may include Suffolk, South Suffolk, and Dorset Down. The bovine hides were from 2–3-year-old cattle of a variety of breeds.

Leathers were generated with a variety of properties using a range of processing parameters during both the conventional beamhouse process and then the conventional tanning of the pelts. Specifically, the pelts were depilated using a caustic treatment comprising sodium sulfide (ranging from a slow-acting paint containing 160 g/L flake sodium sulfide to a quick-acting paint containing 200 g/L sodium sulfide) and a saturated solution of calcium hydroxide. Depilated slats were then processed to remove the residual wool in a solution of sodium sulfide ranging in concentration from 0.8 to 2.4% for 8–16 h at temperatures ranging from 16 to 24 °C. After this treatment, the pelts were washed and treated with a proteolytic enzyme, either a bacterial enzyme (Tanzyme, Tryptec Biochemicals, Ltd.) or a pancreatic enzyme (Rohapon ANZ, Shamrock, Ltd.), at concentrations ranging from 0.025 to 0.1%, followed by pickling in a 2% sulfuric acid and 10% sodium chloride solution. The pickled pelts were then pretanned using oxazolidine, degreased with an aqueous surfactant, and then tanned using chromium sulfate. The resulting "wet blue" was then retanned using a mimosa vegetable extract and impregnated with lubricating oil prior to drying and mechanical softening.

Tear strengths of the crust leathers were tested using standard methods.[18] In brief, samples (strips 1 × 50 mm) were cut from the leather at the official sampling positions (OSPs),[19] parallel to the backbone. The bovine leather was shaved, resulting in samples approximately 1.3 mm thick, consisting, on average, of 34% grain and 66% corium. All samples were then conditioned by storing them at a constant temperature and humidity (20 °C and 65% relative humidity, respectively) for 24 h, after which time they were tested on an Instron strength-testing device.

A stretching apparatus was built as follows. A linear motor, Linmot PS01, 48 × 240/30 × 180-C (NTI AG, Switzerland), was mounted on a purpose-built frame with a custom-made clamp fitted to the end of the slider. The clamp was designed not to put a sharp point load on the leather (Figure 1). A L6D aluminum alloy OIML single-point loadcell (Hangzhou Wanto Precision Technology Co., Zhejiang, China) was attached to a second clamp that would hold the other end of the sample and was attached to the frame.

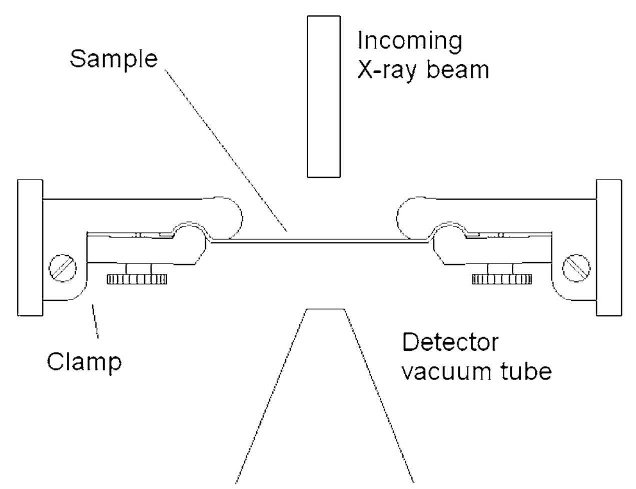

Figure 1. Sketch of the leather-stretching apparatus used for SAXS measurements.

Each leather sample was mounted horizontally between the clamps without tension and then moved into the X-ray beam. The sample was stretched in 1 mm increments until a force was registered by the loadcell. The slider was then moved back 1 mm, so that the sample was again not under tension, and spectra were recorded, with the sample being analyzed edge-on, parallel to the backbone, to allow the load to be correlated with tear strength.[5] Measurements were made, depending upon the mounted orientation of the leather, either normal to the leather surface (flat) in a 0.5 mm grid of four points or edge-on at 0.10 mm intervals across the sample from the grain to the corium. The sample was again stretched 1 mm and maintained at this extension for 1 min to stabilize, before SAXS spectra, the extension, and the force information was recorded. This process was repeated until the sample failed. Note that the flat samples were physically split into two layers, grain and corium, to produce two samples from each piece of leather, before diffraction patterns were recorded.

Diffraction patterns were recorded on the Australian Synchrotron SAXS/WAXS beamline, using a high-intensity undulator source. Energy resolution of 10^{-4} is obtained from a cryo-cooled Si (111) double-crystal monochromator, and the beam size [full width at half maximum (fwhm) focused at the sample] was 250 × 80 μm, with a total photon flux of about 2×10^{12} photons s^{-1}. All diffraction patterns were recorded with an X-ray energy of 11 keV using a Pilatus 1 M detector with an active area of 170 × 170 mm and a sample–detector distance of 3371 mm. Energy calibration used the absorption edge of zinc at 9.659 keV to set the zero angle of the monochromator. This results in energy calibration across the energy range used better than 5 eV and typically better than 2 eV. A diffraction peak of silver behenate is used to scale the camera length. The correct value of q is then calculated by trigonometry for each pixel in each diffraction image. Exposure time for diffraction patterns was 1 s, and data processing was carried out using the SAXS15ID software.[20] No normalization was performed for changes in beam intensity.

Orientation index (OI) is defined as (90° − OA)/90°, where OA is the minimum azimuthal angle range that contains 50% of the microfibrils centered at 180°. OI is used to give a measure of the spread of microfibril orientation (an OI of 1 indicates that the microfibrils are completely parallel to each other, and an OI of 0 indicates that the microfibrils are completely randomly oriented). The OI is calculated from the spread in azimuthal angle of the most intense d-spacing peak (at around 0.059–0.060 Å^{-1}).[5]

The d spacing was determined for each spectrum from Bragg's law by averaging the central values of several collagen peaks (usually from n = 5 to 10).

■ RESULTS

We present here a selection of the data recorded that is representative of the behavior observed in the weak ovine leather (19 or 21 N/mm, normalized for leather cross-section[5]), the stronger ovine leather (39 or 44 N/mm), and in the bovine leather that is stronger still (71 N/mm). An example of a SAXS pattern and the intensity profile are shown in Figure 2. Further details of the data processing may be found in ref 4.

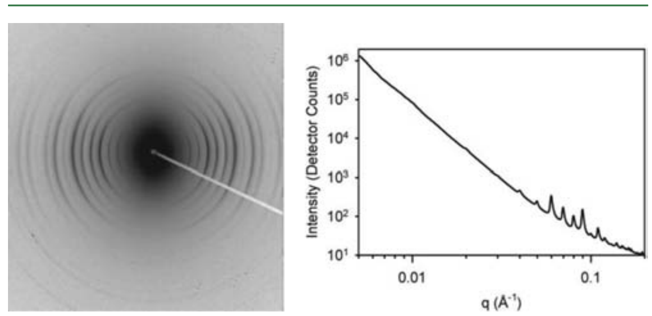

Figure 2. Example of a SAXS pattern of leather (left) and the corresponding intensity profile (right).

Mechanical Properties. Stress response to the applied strain was recorded while the leather samples were mounted edge-on in the SAXS beamline, and strain was applied as

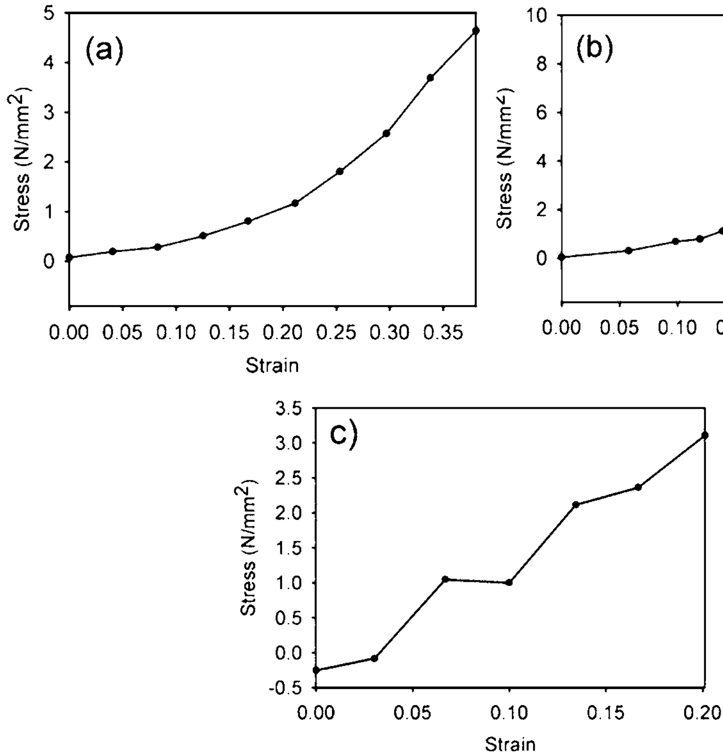

Figure 3. Stress (normalized for the leather cross-section) versus strain (fraction of total unstressed length) curves of leather obtained while SAXS data were collected: (a) weak ovine, 19 N/mm tear strength; (b) stronger ovine, 39 N/mm tear strength; and (c) strong bovine, 71 N/mm tear strength.

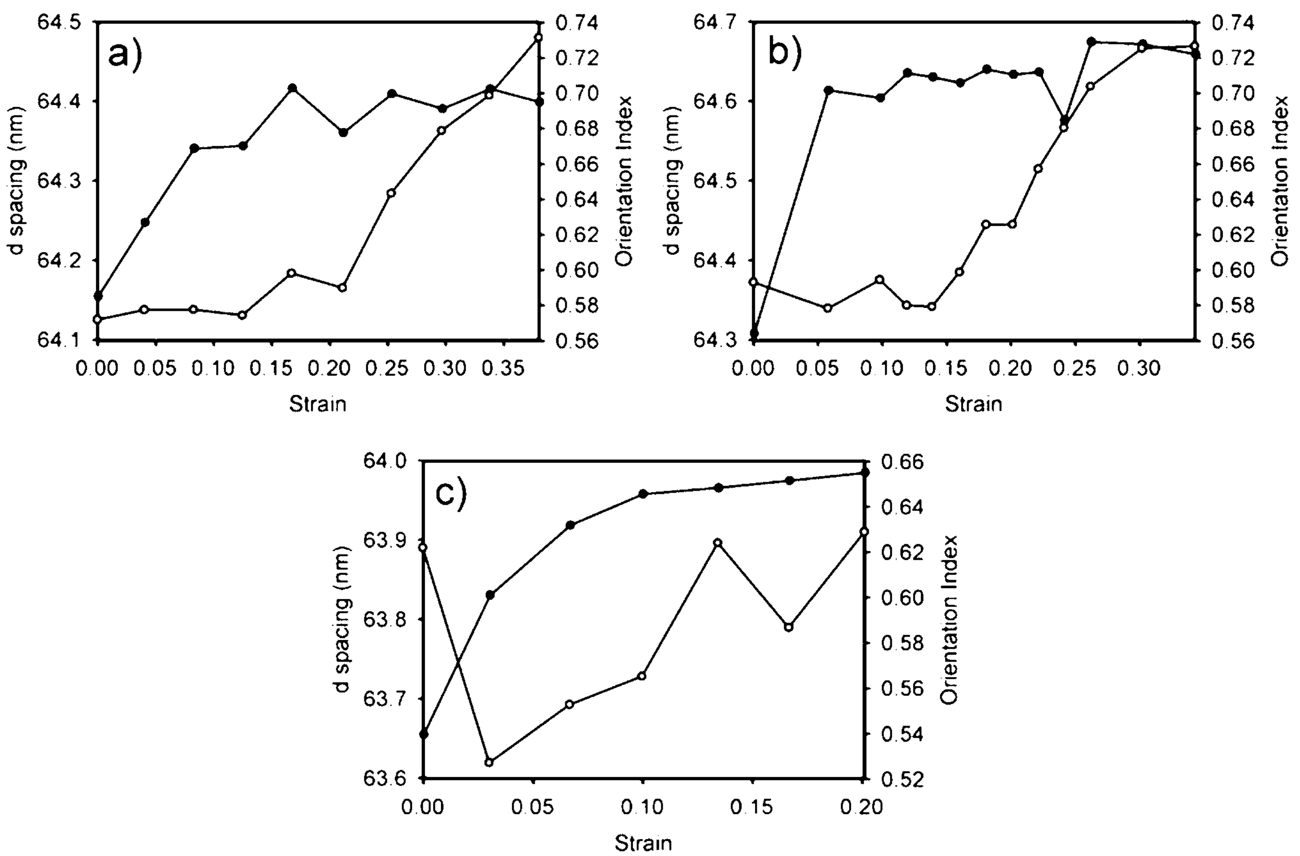

Figure 4. *d* spacing and orientation versus strain measured edge-on, parallel to the backbone: (○) *d* spacing and (●) OI (parallel, OSP) for (a) weak ovine, 19 N/mm tear strength; (b) stronger ovine, 39 N/mm tear strength; and (c) strong bovine, 71 N/mm tear strength.

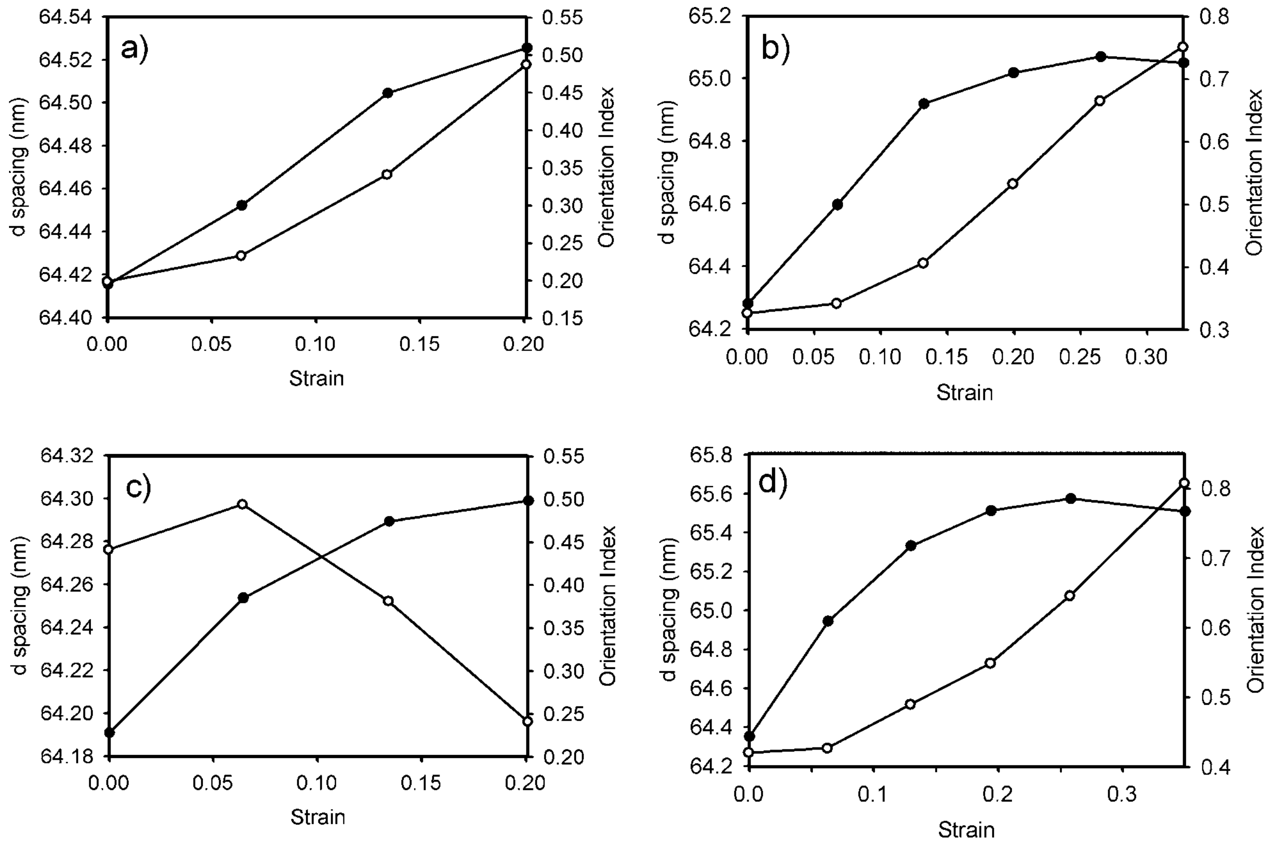

Figure 5. *d* spacing and orientation versus strain measured flat: (○) *d* spacing and (●) OI (parallel, OSP) for (a) weak ovine (21 N/mm tear strength), grain; (b) weak ovine, corium; (c) stronger ovine (44 N/mm tear strength), grain; and (d) stronger ovine, corium.

described in the Experimental Section. The ovine leather became progressively stiffer with stretching, with the slope of the stress strain curve increasing with strain (panels a and b of Figure 3). Qualitatively, the behavior was similar in both weak and stronger ovine leathers. Strong bovine leather did not have such an obvious change in stiffness (Figure 3c), although in the example presented, the strain extended to only 20% (note that strain is dimensionless).

Although the experimental arrangement was not optimized for determining the modulus of elasticity (stiffness) of the leather, it can be obtained from the slope of these plots. The range of the modulus of elasticity was calculated as 2−25 mm^2/N for weak ovine, 5−39 mm^2/N for stronger ovine, and 17 mm^2/N (but only up to 0.20 strain) for strong bovine (panels a, b, and c of Figure 3, respectively). For these leathers, the modulus of elasticity at 0.20 strain was 8, 30, and 15 mm^2/N for weak ovine, stronger ovine, and strong bovine, respectively. These measurements are the tensile stress of very small strips and differ substantially from the tear-strength measurements[18] that are used to determine whether the leather is considered “strong” or “weak”.

Fiber Reorientation and Strain. The OI and *d* spacing were plotted as a function of both strain (Figures 4 and 5) and stress (Figures 6 and 7) to better illustrate the observed structural changes and the causes of these changes.

It is clear that there were complementary changes in the orientation and the *d* spacing. With increasing strain, in the edge-on measured samples, OI increased rapidly at first (i.e., with small strain) and then more slowly at larger strain (above about 0.05−0.08 strain). In contrast, the *d* spacing was almost constant at first before increasing steadily above a threshold of about 0.15−0.20 strain (Figure 4). This strain threshold for *d* spacing increase is similar to that reported for gluteraldehyde-treated bovine pericardium tissue.[15]

With measurement on the flat, the OI was much lower initially than when measured edge-on, but it then increased by a large amount as the leather was stretched (Figure 5). These flat measurements have been shown previously not to be correlated strongly with strength,[5] in contrast to edge-on measurements. However, this direction of measurement has been used in other studies of tissue and leather and, therefore, is included here for comparison, although data for only weak and strong ovine were available. With measurement on the flat, the two-stage process observed in the edge-on samples, where the OI changes with increasing strain first, followed later by a *d*-spacing change, was not as apparent, although there was a larger OI change.

In terms of the stress that the leather experienced, the threshold for OI changes measured edge-on occurred between 0.29 and 0.31 N/mm^2, while significant *d*-spacing changes began at approximately 1.2 N/mm^2 (Figure 6). Within the limitations of the data obtained, stress appears to give a more consistent measure of the thresholds at which changes in structure occur. Although it was expected that the *d* spacing would be a good indicator of structural change with increasing strain, it was less obvious that changes in OI could also predict structural differences.

These changes can be interpreted by the strain initially being taken up by reorientation of the fibrils and fibers, followed by fibril stretching (with less reorientation at this stage). The change in OI gives a quantitative measurement of the rearrangement of the fibers, in this case, with the data indicating that the fibers became more aligned. The change

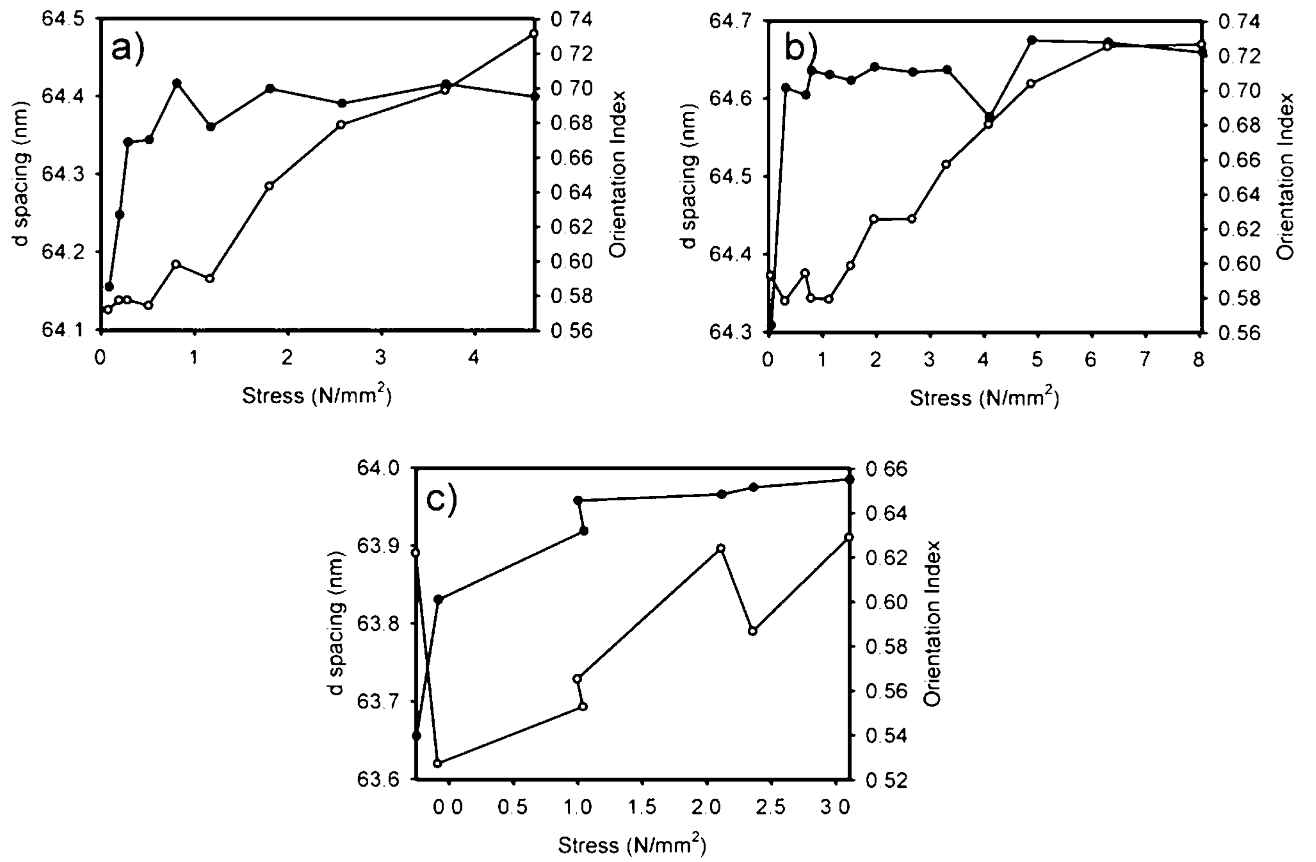

Figure 6. *d* spacing and orientation versus stress measured edge-on parallel to the backbone: (○) *d* spacing and (●) OI (parallel, OSP) for (a) weak ovine, 19 N/mm tear strength; (b) stronger ovine, 39 N/mm tear strength; and (c) strong bovine, 71 N/mm tear strength.

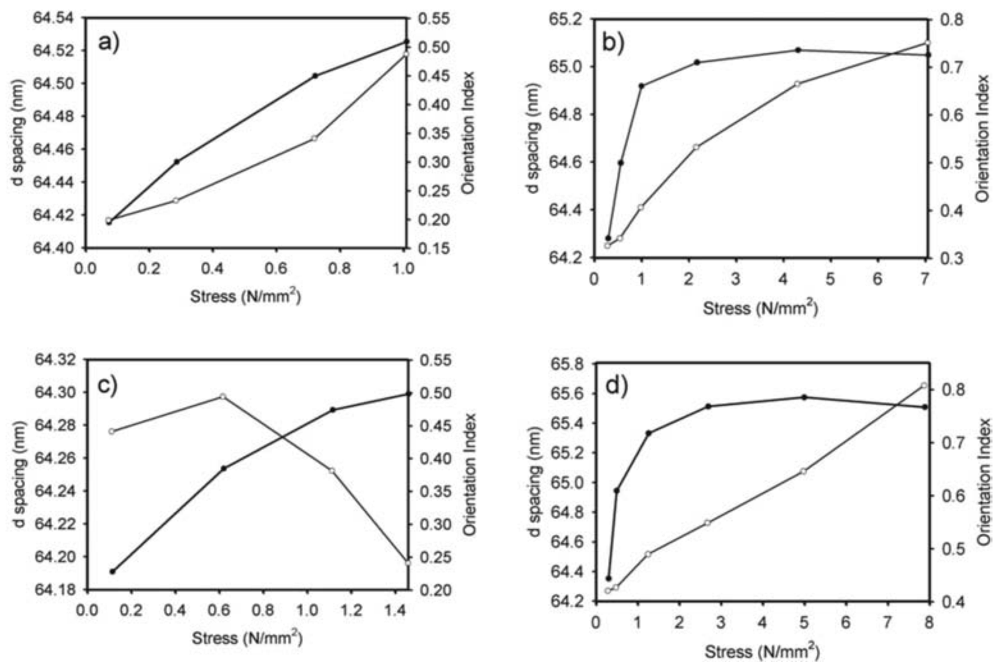

Figure 7. *d* spacing and orientation versus strain measured flat: (○) *d* spacing and (●) OI (parallel, OSP) for (a) weak ovine (21 N/mm tear strength), grain; (b) weak ovine, corium; (c) stronger ovine (44 N/mm tear strength), grain; and (d) stronger ovine, corium.

in *d* spacing is indicative of the strain experienced by individual fibrils as the leather was placed under tension. The decrease in orientation change occurred before the *d* spacing began to significantly increase, indicating that there may be an additional mechanism by which the strain is being distributed to the cross-links that is not apparent from these measurements.[21]

With measurement edge-on, the change observed for OI was very substantial, going from 0.56 to 0.72 for ovine leather and

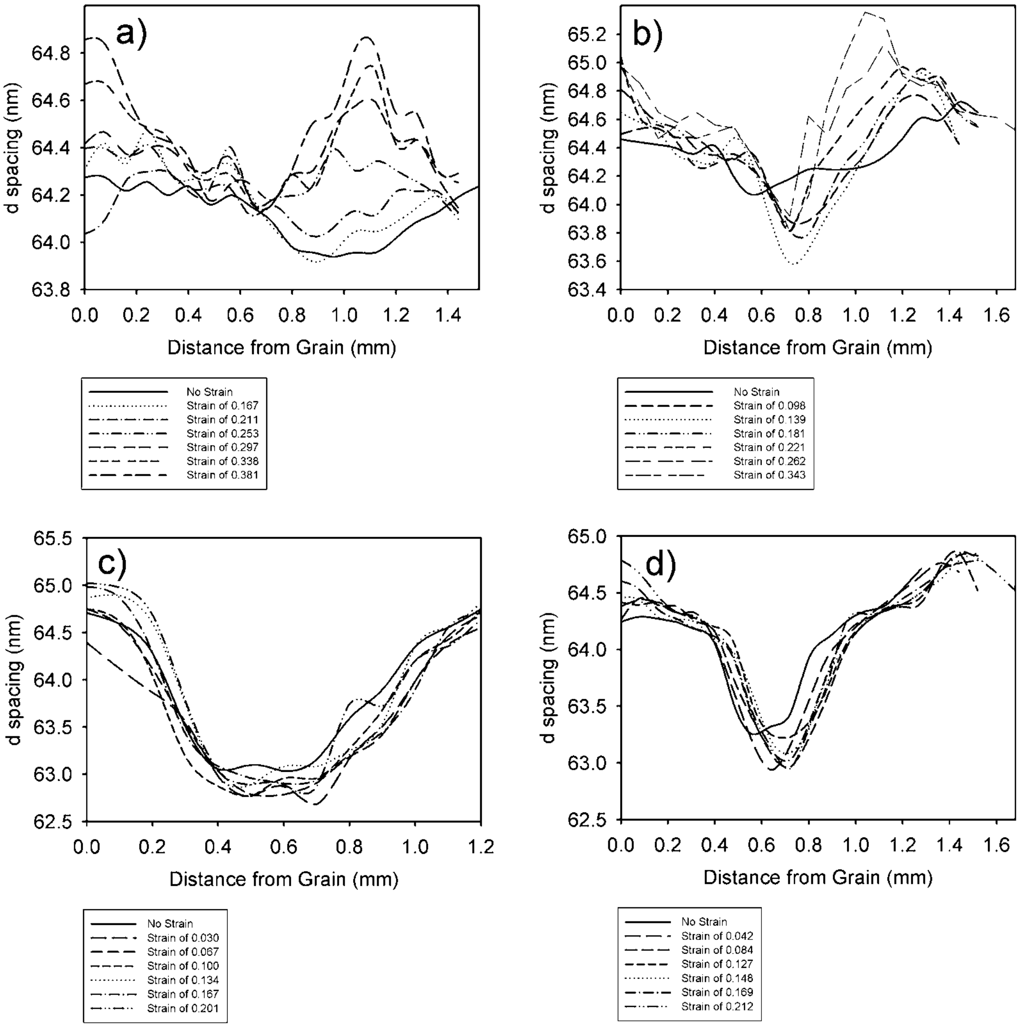

Figure 8. *d* spacing through the thickness of the leather and change in *d* spacing as a consequence of increasing strain, measured edge-on parallel to the backbone for (a) weak ovine, 19 N/mm tear strength; (b) stronger ovine, 39 N/mm tear strength; and (c) strong bovine, 71 N/mm tear strength. Panel d is an example of a second strong ovine leather with a tear strength of 42 N/mm.

from 0.53 to 0.62 for bovine leather (Figure 4). These changes represent a major rearrangement of fibers in the leather. The changes in the *d* spacing were also considerable, with values going from 64.12 to 64.48 nm (or 0.56% extension, with up to 4.6 N/mm^2 stress) for weak ovine skin and from 64.34 to 64.67 nm (or 0.51% extension, with up to 8 N/mm^2 stress) for stronger ovine skin. The *d* spacing continued to change as long as the stress continued to increase.

With measurement on the flat, OI started much lower and underwent a greater change, going from about 0.20 to 0.51 in the grain (panels a and c of Figure 5), from 0.34 to 0.74 in the corium of weak leather (Figure 5b), and from 0.44 to 0.79 in the corium of strong leather (Figure 5d). These changes also represent a major rearrangement of fibers in the leather, although there is not a strong correlation in this direction between strength and orientation.[5] The changes in the *d* spacing are likewise large, with values going from 64.25 to 65.10 nm (or 1.3% extension, with up to 7 N/mm^2 stress) for the corium of weak ovine leather and from 64.27 to 65.65 nm (or 2.1% extension, with up to 7.9 N/mm^2 stress) for the corium of stronger ovine leather. In contrast, in the grain, the increase in *d* spacing was smaller or was reversed (panels a and c of Figure 5).

While the changes in orientation and *d* spacing observed on the flat were greater than those observed edge-on, we believe that the edge-on measurements are of greater significance. It is the extent to which the fibrils are in parallel planes in the leather that determines the strength of the leather (it is the structure measured edge-on that has the most bearing on leather strength); therefore, the change in this structure under tension is of most interest. The quantification of fiber reorientation and stretching in leather during stress is important for developing a model of leather strength.

Cross-sections. SAXS spectra were recorded across the thickness of the leather taken from the OSP and in a direction that was parallel to the direction of the backbone. Previous work has shown that measurements of OI made along this direction are good indicators of strength.[5] The plots of *d* spacing and OI cross-sections (Figures 8 and 9) represent a large number of SAXS spectra and reveal that these parameters vary widely across the thickness of the leather samples and between samples.

For weak ovine leather, the *d*-spacing profile is rather flat when not under tension (Figure 8a), varying by only 0.3 nm and decreasing in the region of the corium. One of the strong ovine leathers showed a similar, fairly flat profile that varied

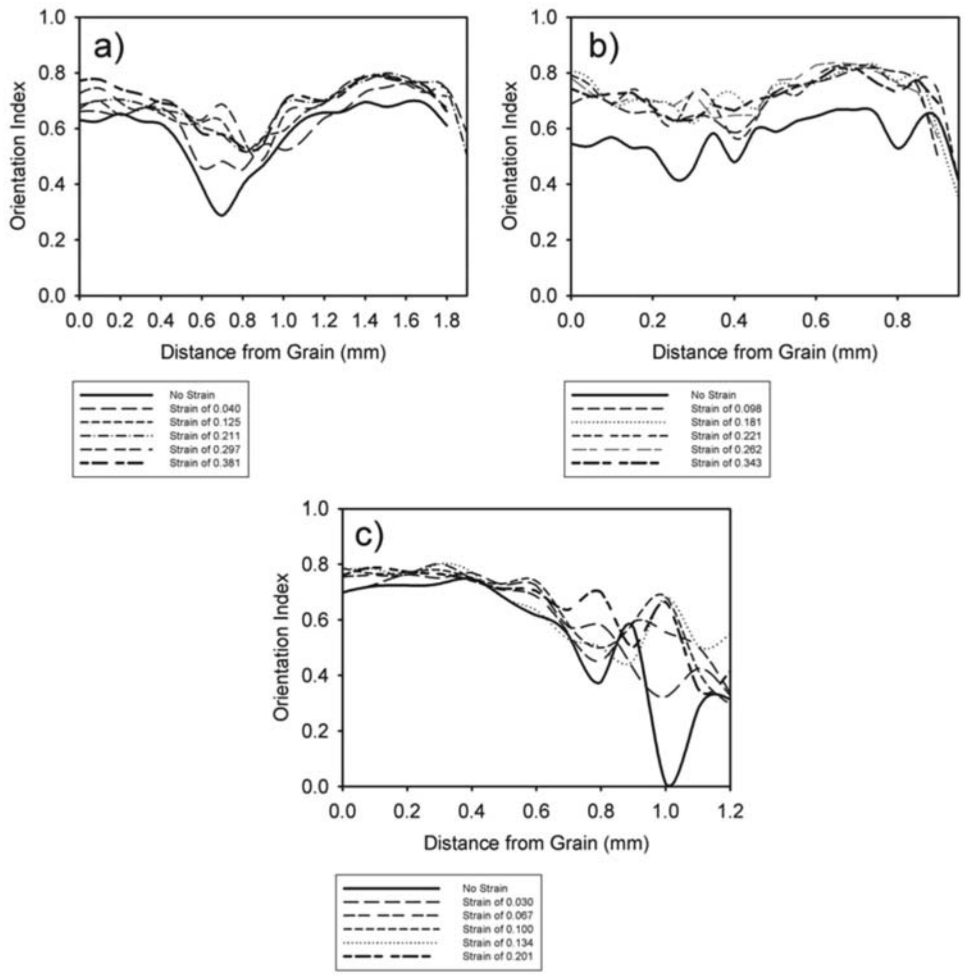

Figure 9. Orientation through the thickness of the leather versus strain and change in orientation as a consequence of increasing strain, measured edge-on parallel to the backbone for (a) weak ovine, 19 N/mm tear strength; (b) stronger ovine, 39 N/mm tear strength; and (c) strong bovine, 71 N/mm tear strength.

only by 0.6 nm at rest. In contrast, the *d* spacing measured for the strongest ovine leather and bovine leathers was lower, at the boundary between the grain and the corium in the middle region, than on either side of this region (panels c and d of Figure 8), decreasing by as much as 1.8 nm for strong ovine and 2.2 nm for strong bovine leather.

Under tension, a markedly different change in *d* spacing was observed for weak ovine leather compared to both strong ovine and bovine leathers. The strain experienced by the fibrils in the weak leather was not uniformly distributed through the leather. Rather, the fibrils remained relatively unstressed in the middle section, while at the surface of the grain and in the bulk of the corium, the *d* spacing increased by up to 1.0 nm as the tension continued to increase. In fact, the profile of the weak ovine leather looked somewhat like that of strong ovine or bovine leather, with a dip in *d* spacing of 0.7 nm at the boundary between the corium and grain (but still less than half that for the strongest ovine or bovine leather). For the strongest ovine and strong bovine leathers, the shapes of the *d*-spacing profiles changed comparatively less when strained and retained the same basic shape throughout (panels c and d of Figure 8). This indicates a chemical and structural difference between strong and weak leathers related to the kind of collagen present, particularly in the corium.

The fibril orientation profiles for all of the ovine leather samples were fairly aligned, except for a slightly less aligned region in the grain close to the grain−corium boundary (panels a and b of Figure 9). In contrast, the fibrils of strong bovine leather were more strongly aligned than those of ovine leather, except at the outer edge of the corium (Figure 9c).

The greatest change in the shape and position of the OI profile occurred during the first one or two increments of stress. During those increases, regions of very low OI were brought generally into line with the rest of the thickness of the leather. The reorientation of fibrils toward greater alignment in the direction of the applied stress took place across the whole thickness of the leather. In addition, fibrils were more uniformly aligned through the whole thickness of the leather during the application of strain than they were before.

These observations provide some evidence of how strain is accommodated in collagen. Leather takes up strain first by reorienting the fibers/fibrils. This happens up to a strain of 15% and a stress of 0.3−0.5 N/mm^2. In the second stage, the fibrils stretch by up to 0.6% before the leather fibers start failing (large pieces of leather under tensile testing fail at strains up to 190%). During the fiber reorientation phase, the leather has a relatively low modulus of elasticity, but once the fibers are highly aligned and begin to individually stretch, the modulus of elasticity rises as the reorientation mechanism is no longer available to the material.

In weak ovine leather, the fibrils across the thickness of the leather are subjected to a much more uneven tensile loading than in either strong ovine or bovine leathers, where the strain is distributed more evenly among the fibrils. This seems to be the most fundamental difference observed between these materials.

In the tear-strength test, which is considered by industry to give a good measure of strength in practical situations, the point of failure occurs at concentrated stress points. It is apparent from this study that the weak ovine leather was not able to spread stress from these concentrated sites throughout the tissue, and therefore, it failed at a lower force. The mechanism for this failure is therefore a progressive rupture of overstressed collagen fibers, leading to a catastrophic breakdown and tear.

This knowledge of the structural basis for strength in leather may lead to new strategies of leather processing and animal breeding to create leather of improved strength.

■ AUTHOR INFORMATION

Corresponding Author

*E-mail: r.haverkamp@massey.ac.nz.

Funding

This work was supported by the Ministry of Science and Innovation, New Zealand (Grant LSRX0801). The Australian Synchrotron provided travel funding and accommodations.

■ ACKNOWLEDGMENTS

This research was undertaken on the SAXS/WAXS beamline at the Australian Synchrotron, Victoria, Australia. Nigel Kirby, David Cookson, Adrian Hawley, and Stephen Mudie at the Australian Synchrotron assisted with data collection and processing. Katie Sizeland and Leah Graham of Massey University also assisted with data collection. Sue Hallas of Nelson assisted with editing the manuscript.

■ REFERENCES

(1) Jian-Bo, Q.; Chuan-Bo, Z.; Jian-Yan, F.; Fu-Tang, G. Natural and synthetic leather: A microstructural comparison. *J. Soc. Leather Technol. Chem.* **2008**, *92*, 8−13.

(2) Haines, B. M. The skin before tannage—Procters view and now. *J. Soc. Leather Technol. Chem.* **1984**, *68*, 57−70.

(3) Floden, E. W.; Malak, S.; Basil-Jones, M. M.; Negron, L.; Fisher, J. N.; Byrne, M.; Lun, S.; Dempsey, S. G.; Haverkamp, R. G.; Anderson, I.; Ward, B. R.; May, B. C. H. Biophysical characterization of ovine forestomach extracellular matrix biomaterials. *J. Biomed. Mater. Res., Part B* **2011**, *96B*, 67−75.

(4) Basil-Jones, M. M.; Edmonds, R. L.; Allsop, T. F.; Cooper, S. M.; Holmes, G.; Norris, G. E.; Cookson, D. J.; Kirby, N.; Haverkamp, R. G. Leather structure determination by small angle X-ray scattering (SAXS): Cross sections of ovine and bovine leather. *J. Agric. Food Chem.* **2010**, *58*, 5286−5291.

(5) Basil-Jones, M. M.; Edmonds, R. L.; Cooper, S. M.; Haverkamp, R. G. Collagen fibril orientation in ovine and bovine leather affects strength: A small angle X-ray scattering (SAXS) study. *J. Agric. Food Chem.* **2011**, *59*, 9972−9979.

(6) Sasaki, N.; Odajima, S. Stress-strain curve and Young's modulus of a collagen molecule as determined by the X-ray diffaction technique. *J. Biomech.* **1996**, *29*, 655−658.

(7) Sasaki, N.; Odajima, S. Elongation mechanisms of collagen fibils and force−strain relations of tendon at each level of structural hierarchy. *J. Biomech.* **1996**, *29*, 1131−1136.

(8) Burger, C.; Zhou, H. W.; Sics, I.; Hsiao, B. S.; Chu, B.; Graham, L.; Glimcher, M. J. Small-angle X-ray scattering study of intramuscular fish bone: Collagen fibril superstructure determined from equidistant meridional reflections. *J. Appl. Crystallogr.* **2008**, *41*, 252−261.

(9) Cedola, A.; Mastrogiacomo, M.; Burghammer, M.; Komlev, V.; Giannoni, P.; Favia, A.; Cancedda, R.; Rustichelli, F.; Lagomarsino, S. Engineered bone from bone marrow stromal cells: A structural study by an advanced X-ray microdiffraction technique. *Phys. Med. Biol.* **2006**, *51* (6), N109−N116.

(10) Goh, K. L.; Hiller, J.; Haston, J. L.; Holmes, D. F.; Kadler, K. E.; Murdoch, A.; Meakin, J. R.; Wess, T. J. Analysis of collagen fibril diameter distribution in connective tissues using small-angle X-ray scattering. *Biochim. Biophys. Acta* **2005**, *1722*, 183−188.

(11) Mollenhauer, J.; Aurich, M.; Muehleman, C.; Khelashvilli, G.; Irving, T. C. X-ray diffraction of the molecular substructure of human articular cartilage. *Connect. Tissue Res.* **2003**, *44*, 201−207.

(12) Fernandez, M.; Keyrilainen, J.; Karjalainen-Lindsberg, M.-L.; Leidenius, M.; Von Smitten, K.; Fiedler, S.; Suortti, P. Human breast tissue characterisation with small-angle X-ray scattering. *Spectroscopy* **2004**, *18*, 167−176.

(13) Liao, J.; Yang, L.; Grashow, J.; Sacks, M. S. The relation between collagen fibril kinematics and mechanical properties in the mitral valve anterior leaflet. *J. Biomech. Eng.* **2007**, *129*, 78−87.

(14) Liao, J.; Yang, L.; Grashow, J.; Sacks, M. S. The relation between collagen fibril kinematics and mechanical properties in the mitral valve anterior leaflet. *J. Biomech. Eng.* **2007**, *129*, 78−87.

(15) Liao, J.; Yang, L.; Grashow, J.; Sacks, M. S. Molecular orientation of collagen in intact planar connective tissues under biaxial stretch. *Acta Biomater.* **2005**, *1*, 45−54.

(16) Sturrock, E. J.; Boote, C.; Attenburrow, G. E.; Meek, K. M. The effect of the biaxial stretching of leather on fibre orientation and tensile modulus. *J. Mater. Sci.* **2004**, *39*, 2481−2486.

(17) Sellaro, T. L.; Hildebrand, D.; Lu, Q. J.; Vyavahare, N.; Scott, M.; Sacks, M. S. Effects of collagen fiber orientation on the response of biologically derived soft tissue biomaterials to cyclic loading. *J. Biomed. Mater. Res., Part A* **2007**, *80A* (1), 194−205.

(18) Williams, J. M. V. IULTCS (IUP) test methods—Measurement of tear load-double edge tear. *J. Soc. Leather Technol. Chem.* **2000**, *84*, 327−329.

(19) Williams, J. M. V. IULTCS (IUP) test methods—Sampling. *J. Soc. Leather Technol. Chem.* **2000**, *84*, 303−309.

(20) Cookson, D.; Kirby, N.; Knott, R.; Lee, M.; Schultz, D. Strategies for data collection and calibration with a pinhole-geometry SAXS instrument on a synchrotron beamline. *J. Synchrotron Radiat.* **2006**, *13*, 440−444.

(21) Chan, Y.; Cox, G. M.; Haverkamp, R. G.; Hill, J. M. Mechanical model for a collagen fibril pair in extracellular matrix. *Eur. Biophys. J.* **2009**, *38*, 487−493.